AIP | Applied Physics Letters

Optical controlled graphene-based nonvolatile ternary-logic transistor with azobenzene copolymer

Chi-Yuan Lin, Chen-Shiung Chang, Jian Hung Lin, Chia-Chen Hsu, and Forest Shih-Sen Chien

Citation: Applied Physics Letters **102**, 013505 (2013); doi: 10.1063/1.4773984
View online: http://dx.doi.org/10.1063/1.4773984
View Table of Contents: http://scitation.aip.org/content/aip/journal/apl/102/1?ver=pdfcov
Published by the AIP Publishing

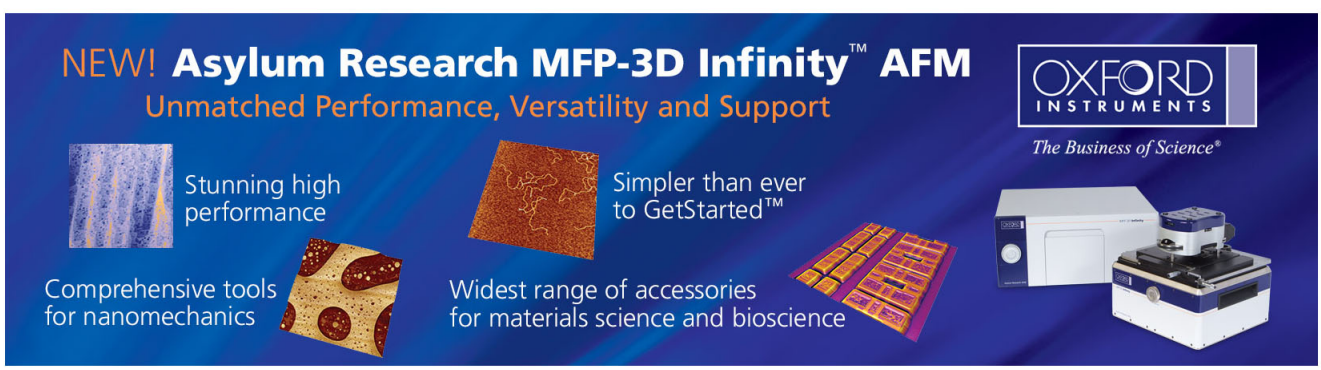

Optical controlled graphene-based nonvolatile ternary-logic transistor with azobenzene copolymer

Chi-Yuan Lin,[1,2] Chen-Shiung Chang,[1,a)] Jian Hung Lin,[3] Chia-Chen Hsu,[3] and Forest Shih-Sen Chien[2,4,a)]
[1]*Department of Photonics and Institute of Electro-Optical Engineering, National Chiao Tung University, Hsinchu 300, Taiwan*
[2]*Department of Physics, Tunghai University, Taichung 407, Taiwan*
[3]*Department of Physics, National Chung Cheng University, Chia Yi 621, Taiwan*
[4]*Tunghai Green Energy Development and Management Institute, Tunghai University, Taichung 407, Taiwan*

(Received 5 October 2012; accepted 17 December 2012; published online 9 January 2013)

We demonstrated optical-controlled graphene-based nonvolatile transistors incorporated with azobenzene copolymer. The transistor was gated by the quasi remnant polarization of azobenzene copolymer, which was built by photo-assisted poling and erased by photo-depoling at room temperature. By taking the nature of polymer electret of azobenzene copolymer, the graphene-based device can perform ternary logic, and the resistance change ratio of the written status "± 1" to the erased status "0" was $\mp 60\%$. The device can retain its statuses against an electric field as high as 0.2 MV/cm because the azobenzene molecules were frozen in copolymer at room temperature. © *2013 American Institute of Physics*. [http://dx.doi.org/10.1063/1.4773984]

Two-dimensional graphene offers the thinnest channel for charge carriers, and thus, graphene field-effect transistors (FETs) can be made with narrower channels and higher speeds than those of Si-based competitors in nanoelectronics.[1] Graphene presents a high-resistance state (R_H) when its Fermi level is near the Dirac point of the conical band structure, and a low-resistance state (R_L) when the Fermi level is far from the Dirac point. The remarkable resistance variation of graphene in response to external electric field has been intensively studied for the applications of electronic devices. Recently, graphene-based bistable transistors are implemented by controlling the hysteretic polarization of ferroelectrics [poly(vinylidene fluoride trifluoroethylene) (PVDF-TrFT)[2–4] or lead-zirconate-titanate (PZT)[5,6]] as ferroelectric random access memories (FRAMs). Such a ferroelectric-gating graphene transistor considers R_H and R_L as statuses "1" and "0," respectively. Unlike unipolar Si-based FRAMs switched by the upward and downward remnant polarizations ($P_\uparrow$ and $P_\downarrow$), ambipolar graphene FETs[7] were switched by minimal and maximal remnant polarizations of ferroelectrics. Therefore, the reversible switching between R_H and R_L is performed by two different asymmetric sweeps of gate bias to build the necessary remnant polarizations for each state.[2] Otherwise, in addition to ferroelectric gating, a normal dielectric backgating (so called dual-gating) would be necessary to introduce a reference background doping in graphene for symmetrical bit writing.[3] Therefore, it is desirable to design graphene-based transistors with a straightforward switching scheme.

Optical methods could offer some practical solutions to the gating issue of graphene transistors. For instance, a nonvolatile graphene/polymer memory was demonstrated, in which a layer of poly(methyl styrene-*co*-chloromethyl acrylate) (ZEP520A) acts as a floating gate. Under illumination of UV light, ZEP520A turns into an electron acceptor due to photochemical reaction, and after annealing above glass temperature (170 °C), ZEP520A is restored to its original status prior to UV exposure.[8] Recently, pyrene-tethered disperse red one (DR1P) has been used to optically modulate the conduction of carbon nanotubes and graphene.[9,10] DR1P chromophores are tethered to graphene via π-π interactions. The optical-reactive polar disperse red one (DR1) is a derivative of the azobenzene chromophore with an appreciable permanent dipole moment and nonlinear polarizability. Under illumination by the light of proper wavelengths, DR1 undergoes the reversible *trans* ↔ *cis* photo-isomerization cycles. A *trans* isomer has a higher dipole moment than a *cis* one does. The doping in carbon nanotubes or graphene is changed due to the dipole moment contrast between *trans* and *cis* isomers of DR1P. However, the response time of DR1P is as long as 10^3 s and the resistance change ratio $[(R_H-R_L)/R_L]$ is only 10%.

Polar and nonlinear-optics DR1-containing polymers and copolymer have been demonstrated to have many possible optical applications, e.g., optical storage,[11–13] second harmonic generation,[14,15] and switch/modulator.[16–18] The copolymers of DR1 and polymethylmethacrylate (DR1-PMMA) have the backbone of PMMA with the covalently bonded side chains of DR1. DR1-PMMA is an optical-reactive polymer electrets. The polar orientation of DR1 chromophores can be built by photo-assisted poling (PAP) and erased by photo-depoling (PD).[19–22] In this paper, we adopted optical-reactive DR1-PMMA copolymers as the active materials in graphene-based nonvolatile transistors, which were operated by a simple polarization-gating scheme. This study examined the dependence of graphene resistance on the operations of PAP and PD. The status of the graphene/DR1-PMMA device can be written by PAP with a simple step-like bias, and erased by PD, both at room temperature. The substitution of azobenzene copolymers for DR1P chromophores significantly improved the performance of the graphene devices in the response time and resistance change ratio. A ternary logic can be performed with the graphene/DR1-PMMA FET. This study also demonstrated

a)Authors to whom correspondence should be addressed. Electronic addresses: cschang@mail.nctu.edu.tw and fsschien@thu.edu.tw.

the robustness of the device in the presence of a strong electric field.

In this work, graphene sheets were prepared on SiO_2/Si substrates by mechanical exfoliation.[23] The thickness of SiO_2 was 300 nm to have the graphene visible under the inspection of optical microscope. The exfoliated graphene had been verified to be few layers by micro Raman spectroscopy.[24] The schematic of the graphene/DR1-PMMA device is shown in Fig. 1(a). The source and drain electrodes on the graphene sheet were fabricated by evaporating Ti/Au (5 nm/10 nm). The thin layer of DR1-PMMA copolymer was sandwiched between the graphene and transparent conductive layer of indium tin oxide (ITO). The commercial DR1-PMMA copolymer (ALDRICH 570435) was dissolved in chloroform with 3.3 wt. %, filtered with a 250 nm filter, and spin-coated on graphene at 500 rpm. The DR1-PMMA film was subsequently heated to 80 °C for 30 min to remove the chemical solvent. The thickness of the copolymer film was approximately 1 μm, measured by atomic force microscopy at a scratched edge. The peak absorption wavelength of the DR1-PMMA film was approximately 470 nm,[15] and the light source for pumping was a 479 nm linear-polarized diode-pumped solid-state laser. The top ITO electrode was deposited on DR1-PMMA by sputtering, to apply the poling bias (V_P) for PAP. The Si substrate was used as the bottom electrode to apply the gate bias (V_G). V_G was only for measuring the curves of resistance (R) vs. V_G of the graphene channel. The bottom electrode was not used to the writing and erasing operations of the graphene/DR1-PMMA FET. The resistance of the device was characterized at ambience.

The switching scheme of the graphene/DR1-PMMA FET by PAP and PD is shown in Fig. 1. The normal-incident pumping laser is applied from the top of the device, where the polarization of laser is parallel to the sample surface. DR1 has the ground-state *trans* isomer and the excited-state *cis* isomer. The *trans*-state DR1 possesses an extremely low angular mobility below the glass temperature (T_g),[20,25] so *trans*-state DR1 does not rotate under electric field (i.e., DR1 has no coercive field). A pumping light and V_p are simultaneously applied to DR1-PMMA to activate the PAP process. The pumping laser induces the cycles of *trans* ↔ *cis* photoisomerization to DR1. The probability of pumping is proportional to $\cos^2\theta$, where θ is the angle between the dipole moment of DR1 and the polarization of pumping laser. However, the angular mobility of the *cis* DR1 is high enough to permit DR1 to align in the direction of poling field during the lifetime of *cis* state (even the temperature is below T_g).[20,25] A partial memory of the orientation (parallel to the poling field) retains after the *cis* → *trans* back reaction under the poling field. Therefore, the polar orientation of DR1 chromophores (so as the quasi-remnant polarization) can be optically built by PAP.[19–22] When a positive V_P and laser illumination are applied simultaneously, a $P_\downarrow$ in DR1-PMMA is built after the PAP process [Fig. 1(a)]. The Fermi level of graphene is upshifted because of the accumulation of negative charges in graphene induced by $P_\downarrow$.

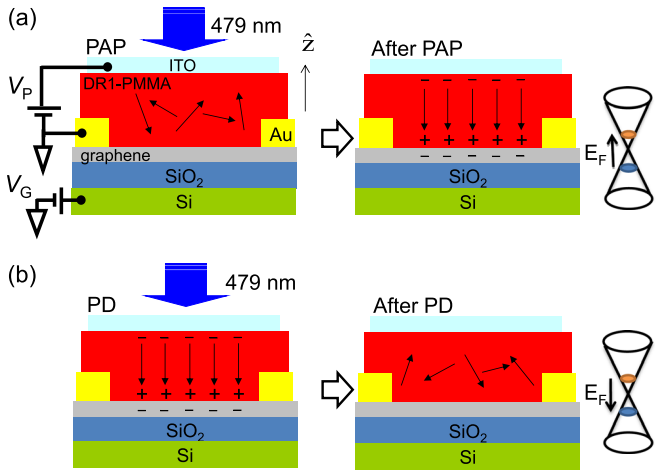

FIG. 1. (a) Operation of PAP by a *positive* poling bias to build the *downward* quasi-remnant polarization ($P_\downarrow$) in the graphene/DR1-PMMA device and cause the upshift of Fermi level (E_F) correspondingly. The arrow represents the orientation of the dipole moment of a DR1 chromophore. The laser illumination was applied from the top. (b) Operation of PD to erase the built $P_\downarrow$ and return E_F to its original level.

To erase the PAP-induced P, the poled DR1-PMMA is illuminated by the same laser without poling bias [Fig. 1(b)].[19] The polar orientation of DR1 is randomized (referred to as PD), because DR1 loses its memory of orientation after several *trans* ↔ *cis* cycles under laser illumination. Circular- or non-polarized laser is more efficient in randomizing polar orientation, but the same linearly polarized laser was applied in PD to simplify the experimental configuration. The Fermi level of graphene resumes its initial position after the PD process. The optical control of P in DR1-PMMA by PAP and PD is repeatable.

The operational mechanism of graphene/DR1-PMMA devices is intrinsically different from that of graphene/DR1P. For the graphene/DR1P device, a UV light is applied to produce the *trans* → *cis* reaction, and a white light to the *cis* → *trans*.[10] The resistance change of graphene/DR1P devices is induced by the dipole moment difference between *trans* and *cis* DR1P isomers. In our scheme, the resistance change is induced by the polarization difference between the poled and depoled DR1-PMMAs. PAP and PD are employed to build and erase polarization. Only one light source is required for both PAP and PD.

In this study, a 14 mW/cm^2 laser was applied to illuminate the graphene/DR1-PMMA transistor for 10 s to activate the PAP process. Such a laser exposure was not enough to induce mass transport in DR1-PMMA. During PAP, V_P could also induce the resistance change of graphene. To avoid confusing the role of V_P, we intentionally plot the curves of R vs. V_G in Fig. 2(a) to show the response of the curves to PAP and PD. The resistance of the graphene reached a maximum value (R_{MAX}) as its Fermi level reached the Dirac point. V_{MAX} is denoted as the V_G at R_{MAX}. Before any PAP process, V_{MAX} was 5 V because of the dopant concentration (n_{env}) induced by the ambient dielectric environment, where $n_{env} = C_{SiO_2}V_{MAX}/e = 3.59 \times 10^{11}$ cm^{-2} ($C_{SiO_2} = 1.15 \times 10^{-8}$ F/cm^2, the gate capacitance per unit area of SiO_2). The carrier mobility $\mu = (eR_S n_{env})^{-1}$ was as high as 2400 cm^2 V^{-1} s^{-1},[7,26] where R_S is the sheet resistance of graphene. When R was close to its minimum, the total carrier concentration n_T was as high as 7.4×10^{11} cm^{-2} in graphene.

The PAP-induced P caused the change in carrier concentration of graphene, resulting in the shift of resistance curves.

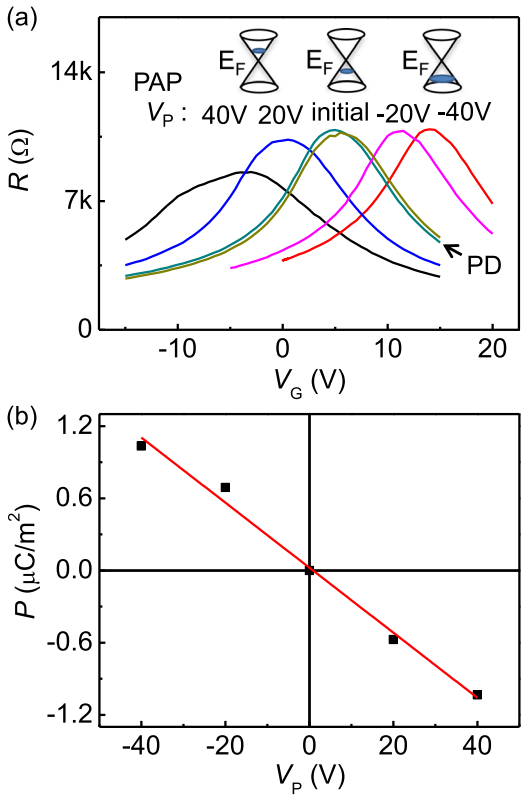

FIG. 2. (a) Resistance of a graphene/DR1-PMMA device varied with the gating bias V_G. The curve of resistance was shifted after PAP. The magnitude of the shift was proportional to the poling bias V_P of PAP. The curve returned to its initial status after PD, indicated by an arrow at the lower right corner. The Fermi level before and after PAP is schematically shown above the curves. (b) Dependence of PAP-induced polarization in the DR1-PMMA on V_P, derived by the shift of resistance curves (i.e., the shift of V_{MAX}) with respect to V_P with Eq. (2).

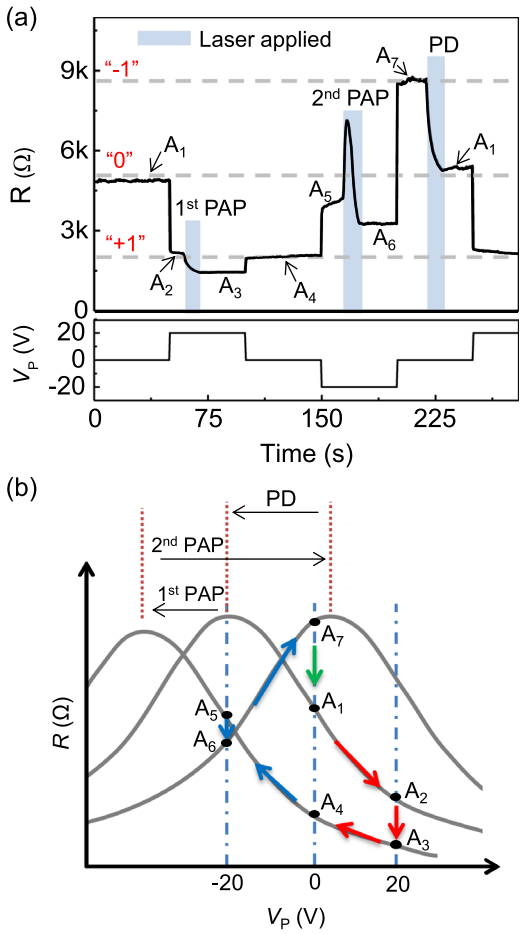

FIG. 3. (a) (Upper panel) Temporal response of the resistance of a graphene/DR1-PMMA transistor to PAP and PD, and (lower panel) the concurrent poling bias V_P. The resistance of the device was denoted by positions A_1 to A_7. The blue stripes indicate when the illumination was applied for the 1st PAP (A_2 to A_3), 2nd PAP (A_5 to A_6), and PD (A_7 to A_1). Positions A_1, A_4, and A_7 represent the statuses "0," "+1," and "−1." (b) Schematic of the variation of resistance from positions A_1 to A_4 with the 1st PAP denoted by the red arrows, from A_4 to A_7 with the 2nd PAP denoted by the blue arrows, and from A_7 to A_1 with the PD denoted by the green arrow. V_P followed the step-like path in lower panel of Fig. 3(a). The black arrows above the curves indicate that the curve shifted to the left with the 1st PAP, to the right with the 2nd PAP, and to the left again back to its initial status with PD.

P is a function of V_P,[27] so the shift became larger as $|V_P|$ increased as shown in Fig. 2(a). As a positive (negative) V_P was applied for PAP, the resistance curve shifted to the left (right) due to the induced $P_\downarrow$ ($P_\uparrow$). Note that we observed no hysteretic response with the device up to $|V_P| = \pm 15$ V without laser illumination. As $|V_P| = \pm 20$ V, hysteretic response occurred, where V_{MAX} shifted by 4 V due to the trapped charges at interface. Therefore, the polarization of DR1-PMMA was the main contribution to the shift of the resistance curve, but not the interface trapping or de-trapping charge carriers in the ferroelectric gating graphene/PZT FET.[5,6] Finally, P was removed by PD and the resistance curve returned to its initial status.

For the continuity of the displacement field at the graphene/DR1-PMMA interface, we have the expression for n_T

$$n_T e = -C_{SiO_2} \cdot (V_G - V_0) + \vec{P} \cdot \hat{z}, \tag{1}$$

where V_0 (=5 V) is the V_{MAX} associated with n_{env} and $\hat{z}$ is the unit vector of the upright direction. R_{MAX} occurred when

$$\vec{P} \cdot \hat{z} = C_{SiO_2} \cdot (V_{MAX} - V_0). \tag{2}$$

Hence, the relation between P and V_P was obtained, as shown in Fig. 2(b). P was found to depend linearly on V_P. The P induced by $V_P = \pm 40$ V was approximately one-tenth of the remnant polarization of typical ferroelectric ceramics ($SrBi_2Ta_2O_9$).[28]

The temporal resistance response of the graphene/DR1-PMMA transistor to PAP and PD is shown in Fig. 3(a). The processes included a positive-biased PAP, a negative-biased PAP, and a PD. Initially, the device was denoted as status "0" and its resistance $R_0 = 5$ kΩ. The first PAP was executed with $V_P = +20$ V. The resistance followed the path from positions A_1 to A_4; A_1 to A_2 along the curve for the field effect of applied V_P, A_2 to A_3 for the left shift of the curve caused by the PAP-induced $P_\downarrow$ under laser illumination, and A_3 to A_4 along the left-shifted curve for the release of V_P. Figure 3(b) schematically shows the variation of resistance in response to PAPs, in the R vs. V_P representation. Note that V_P followed the step-like path at the lower panel of Fig. 3(a), instead of a zigzag path. At A_4 (where $V_P = 0$), the resistance change from A_1 to A_4 was only attributed to P. The device was latched to A_4, denoted as status "+1," and its resistance $R_{+1} = 2$ kΩ. Subsequently, the second PAP was executed with

$V_P = -20$ V. The resistance followed the path from A_4 to A_7, similar to the sequence from A_1 to A_4 with the first PAP except that the curve shifted to the right because of the $P_\uparrow$. While the curve was shifting to the right during the second PAP, the resistance passed through R_{MAX} and a spike of resistance appeared between A_5 and A_6. The device was latched to a new position A_7, denoted as status "−1" after the second PAP, and its resistance $R_{-1} = 8.5\,k\Omega$. Finally, the resistance returned to the initial position A_1 after the execution of a PD process, i.e., the status "−1" was switched to "0." The graphene/DR1-PMMA device can easily perform ternary logic by PAP "±1" and PD for "0." A ternary memory has the advantage of higher data storage capacities and faster processing over the traditional binary memory.[29,30] Unlike graphene/ferroelectric transistors requiring asymmetric bias sweeps or dual-gate designs,[2,3] graphene/DR1-PMMA FETs are operated by simple illumination and bias. Because the polarization of DR1 can be repeatedly built and erased by the PAP and PD process, this nonvolatile ternary transistor is rewritable. With other ferroelectric materials, it is very difficult to perform ternary logic because erasing P of ferroelectrics requires many hysteretic loops.

From Fig. 3(a), the response time of graphene/DR1-PMMA devices to PAP is less than 10 s. Compared with graphene/DR1P devices whose response time is $\sim 10^3$ s,[10] graphene/DR1-PMMA devices show a significant improvement in response time, because the angular reorientation was accelerated by poling field. There are several approaches to further improve the response time of azobenzene copolymers, e.g., to enhance the permanent dipole moment of chromophores by tailoring the functional groups, to reduce the pumping time by increasing the quantum yield,[20] and to increase the poling field by thinning the copolymer films. The resistance change ratio ($|R_{\pm 1} - R_0|/R_0$) is approximately 60%. The overall ratio ($|R_{-1} - R_{+1}|/R_{+1}$) is 325%. Compared with the ratio of graphene/DR1P devices (10%), the resistance change is remarkably improved, because the change was contributed to the polarization difference between the poled DR1-PMMA and the depoled DR1-PMMA. On the other hand, the areal density of the proposed devices under its present scheme is restricted by the diffraction limit. To overcome this limitation and increase the density, some more advanced scanning-probe approaches can be adopted, e.g., to induce nano-movement of azo copolymers by enhanced near-field irradiation[31] and to perform local PAP with scanning probes in azo copolymer.[27]

The polar orientation of *trans* DR1 in copolymer is frozen at a temperature below T_g, because rigid polymer main chains hinder the angular motion of DR1. Previous studies[32,33] showed the long-term stability of the polar orientation of the poled DR1-PMMA copolymer by PAP below T_g. This unique feature allows graphene/DR1-PMMA transistors to withstand the influences of strong electric fields when no illumination is applied. To verify the robustness of the device against electric field, the graphene/DR1-PMMA device (both statuses "0" and "+1") experienced a strong electric field without illumination. A loop of V_P ($0\,V \leftrightarrow -20\,V$) was applied to the device at status "0" without illumination. The status was firmly preserved as its resistance went through a cycle ($B_1 \leftrightarrow B_2$) (Fig. 4). Then, the device was switched to status "+1" by PAP. The same loop of V_P was reapplied

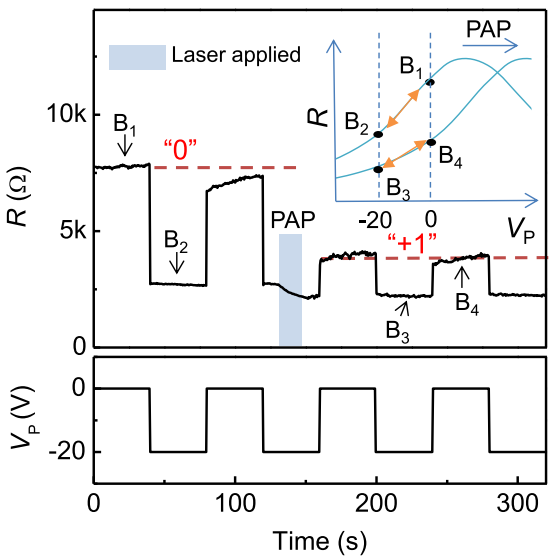

FIG. 4. (Upper panel) Temporal response of the resistance of a graphene/DR1-PMMA transistor against the loops of V_P ($0 \leftrightarrow -20$ V) without illumination to show the robustness of statuses "0" and "+1," and (lower panel) the concurrent loops of V_P. The PAP was applied to write the status "+1." The inset is to illustrate the variation of resistance of the device in response to the loop of V_P at statuses "0" and "+1."

without illumination. The status "+1" was also preserved after a cycle of resistance ($B_3 \leftrightarrow B_4$). These results demonstrated the robustness of the device to an external electric field as high as 0.2 MV/cm, which is higher than the coercive field of conventional ferroelectrics (0.1 MV/cm).[28]

Because of their intrinsic limitations, the graphene/DR1-PMMA devices cannot outperform the solid-state ferroelectric-gating devices in many aspects.[2,3] The PAP and PD involved the molecular motion, which is slow (approximately the order of milliseconds) compared with the solid-state devices. The writing/erasing operation time of graphene/DR1-PMMA devices is restricted. In addition, the areal density of the devices is restricted by diffraction limit due to the optical controlled processes with the present scheme. Furthermore, fatigue and degradation of organic materials result in a shorter endurance and lifetime of the devices than those of solid-state devices. However, graphene/DR1-PMMA devices are compatible with the non-expensive yet high-throughput spin coating processes, so the devices are able to be integrated into flexible organic devices. There are many occasions to which graphene/DR1-PMMA devices are applicable. For example, low-cost disposable radio-frequency identification (RFID) tags need write-once read-many memories, which request low levels of speed, capacity, and endurance. Therefore, graphene/DR1-PMMA devices are the potential candidate for disposable RFID tags.

In summary, we demonstrated a rewritable graphene-based nonvolatile ternary-logic transistor, which was incorporated with optical-reactive DR1-PMMA copolymer. The graphene/DR1-PMMA transistor was controlled optically by a simple scheme of illumination and bias at room temperature. The resistance curve of graphene was shifted because of doping induced by the quasi-remnant polarization of DR1-PMMA. Repeatedly, the status of the device was written to "+1"/"−1" simply with the downward/upward remnant polarization built by a positive/negative-biased PAP, and the status

was erased to be "0" as the polarization was removed by PD. The resistance change ratio of the written status "± 1" to the erased status "0" was $\mp 60\%$. The graphene/DR1-PMMA transistor can withstand an electric field as high as 0.2 MV/cm because DR1-PMMA is a robust polymer electret without a coercive field below glass temperature.

The authors gratefully acknowledge the financial support of the Project of Global Research & Education on Environment and Society, Tunghai University and the National Science Council, Taiwan, under Grant Nos. NSC 99-2112-M-029-005-MY3 and NSC 98-2112-M-009-012-MY3.

[1]F. Schwierz, Nat. Nanotechnol. **5**, 487 (2010).
[2]Y. Zheng, G.-X. Ni, C.-T. Toh, M.-G. Zeng, S.-T. Chen, K. Yao, and B. Özyilmaz, Appl. Phys. Lett. **94**, 163505 (2009).
[3]Y. Zheng, G.-X. Ni, C.-T. Toh, C.-Y. Tan, K. Yao, and B. Özyilmaz, Phys. Rev. Lett. **105**, 166602 (2010).
[4]Y.-J. Doh and G.-C. Yi, Nanotechnology **21**, 105204 (2010).
[5]X. Hong, J. Hoffman, A. Posadas, K. Zou, C. H. Ahn, and J. Zhu, Appl. Phys. Lett. **97**, 033114 (2010).
[6]E. B. Song, B. Lian, S. M. Kim, S. Lee, T.-K. Chung, M. Wang, C. Zeng, G. Xu, K. Wong, Y. Zhou, H. I. Rasool, D. H. Seo, H.-J. Chung, J. Heo, S. Seo, and K. L. Wang, Appl. Phys. Lett. **99**, 042109 (2011).
[7]K. S. Novoselov, A. K. Geim, S. V. Morozov, D. Jiang, Y. Zhang, S. V. Dubonos, I. V. Grigorieva, and A. A. Firsov, Science **306**, 666 (2004).
[8]S. Lara-Avila, K. Moth-Poulsen, R. Yakimova, T. Bjørnholm, V. Fal'ko, A. Tzalenchuk, and S. Kubatkin, Adv. Mater. **23**, 878 (2011).
[9]J. M. Simmons, I. In, V. E. Campbell, T. J. Mark, F. Léonard, P. Gopalan, and M. A. Eriksson, Phys. Rev. Lett. **98**, 086802 (2007).
[10]M. Kim, N. S. Safron, C. Huang, M. S. Arnold, and P. Gopalan, Nano Lett. **12**, 182 (2012).
[11]Z. Sekkat, J. Wood, W. Knoll, W. Volksen, R. D. Miller, and A. Knoesen, J. Opt. Soc. Am. B **14**, 829 (1997).
[12]G. Xu, Q. G. Yang, J. Si, X. Liu, P. Ye, Z. Li, and Y. Shen, Opt. Commun. **159**, 88 (1999).
[13]D. Gindre, A. Boeglin, A. Fort, L. Mager, and K. D. Dorkenoo, Opt. Express **14**, 9896 (2006).
[14]G. Martin, S. Ducci, R. Hierle, D. Josse, and J. Zyss, Appl. Phys. Lett. **83**, 1086 (2003).
[15]J. H. Lin, N. D. Lai, C. H. Chiu, C.-Y. Lin, G. W. Rieger, J. F. Young, F. S.-S. Chien, and C. C. Hsu, Opt. Express **16**, 7832 (2008).
[16]M.-H. Lee, Y. H. Min, J. J. Ju, J. Y. Do, and S. K. Park, IEEE J. Sel. Top. Quantum Electron. **7**, 812 (2001).
[17]A. Donval, E. Toussaere, R. Hierle, and J. Zyss, J. Appl. Phys. **87**, 3258 (2000).
[18]J. H. Lin, Y. C. Huang, N. D. Lai, H.-C. Kan, and C. C. Hsu, Opt. Express **20**, 377 (2012).
[19]P. M. Blanchard and G. R. Mitchell, J. Phys. D: Appl. Phys. **26**, 500 (1993).
[20]Z. Sekkat and W. Knoll, J. Opt. Soc. Am. B **12**, 1855 (1995).
[21]S. Bauer, J. Appl. Phys. **80**, 5531 (1996).
[22]Y. Atassi, J. Chauvin, J. A. Delaire, J.-F. Delouis, I. Fanton-Maltey, and K. Nakatani, Pure Appl. Chem. **70**, 2157 (1998).
[23]K. S. Novoselov, D. Jiang, F. Schedin, T. J. Booth, V. V. Khotkevich, S. V. Morozov, and A. K. Geim, Proc. Natl. Acad. Sci. U.S.A. **102**, 10451 (2005).
[24]A. C. Ferrari, J. C. Meyer, V. Scardaci, C. Casiraghi, M. Lazzeri, F. Mauri, S. Piscanec, D. Jiang, K. S. Novoselov, S. Roth, and A. K. Geim, Phys. Rev. Lett. **97**, 187401 (2006).
[25]R. A. Hill, S. Dreher, A. Knoeson, and D. R. Yankelevich, Appl. Phys. Lett. **66**, 2156 (1995).
[26]A. K. Geim and K. S. Novoselov, Nat. Mater. **6**, 183 (2007).
[27]F. S.-S. Chien, C. Y. Lin, C. R. Huang, C. S. Chang, and C. C. Hsu, J. Opt. Soc. Am. B **27**, 773 (2010).
[28]H. Ishiwara, M. Okuyama, and Y. Arimoto, *Ferroelectric Random Access Memories Fundamentals and Applications* (Springer-Verlag, Berlin Heidelberg, 2004), Chap. 1.
[29]B. Hayes, Am. Sci. **89**, 490 (2001).
[30]I. Lebar Bajec, N. Zimic, and M. Mraz, Nanotechnology **17**, 1937 (2006).
[31]H. Ishitobi, M. Tanabe, Z. Sekkat, and S. Kawata, Appl. Phys. Lett. **91**, 091911 (2007).
[32]Z. Sekkat and M. Dumont, Mol. Cryst. Liq. Cryst. Sci. Technol., Sect. B: Nonlinear Opt. **2**, 359 (1992).
[33]G. A. Lindsay and K. D. Singer, *Polymers for Second-Order Nonlinear Optics* (American Chemical Society, Washington, DC, 1995), Chap. 19.